

ANALYSIS OF FAST ATTACK CRAFT RUDDER FAILURE

Amune Hene Gedara Pradeep Nishantha Gunarathna

118556 G



University of Moratuwa, Sri Lanka.
Electronic Theses & Dissertations
Degree of Master of Science
www.lib.mru.ac.lk

Department of Materials Science and Engineering

University of Moratuwa
Sri Lanka

April 2016

ANALYSIS OF FAST ATTACK CRAFT RUDDER FAILURE

Amune Hene Gedara Pradeep Nishantha Gunarathna

118556 G



University of Moratuwa, Sri Lanka.
Electronic Theses & Dissertations
www.lib.mrt.ac.lk

Dissertation submitted in partial fulfillment of the requirements for the
degree Master of Science in Material Science

Department of Materials Science and Engineering

University of Moratuwa

Sri Lanka

April 2016

DECLARATION

I declare that this is my own work and this dissertation does not incorporate without acknowledgement any material previously submitted for a Degree or Diploma in any other University or institute of higher learning and to the best of my knowledge and belief it does not contain any material previously published or written by another person except where the acknowledgement is made in the text.

Also, I hereby grant to University of Moratuwa the non-exclusive right to reproduce and distribute my dissertation, in whole or in part in print, electronic or other medium. I retain the right to use this content in whole or part in future works (such as articles or books).

Signature:

Date:

The above candidate has carried out research for the partial fulfillment of the requirements for the Degree Master of Science in Materials Science under my supervision.



University of Moratuwa, Sri Lanka
Electronic Theses & Dissertations
www.lib.mrt.ac.lk

Name of the supervisor: Eng. S.P. Guluwita

Signature of the supervisor:

Date:

Abstract

It is observed that frequent rudder failures of Sri Lanka Navy's fast attack craft which are equipped with conventional propulsion system. Therefore, it was unable to effectively utilize these craft for operational requirements in the Navy.

In this research it was analyzed both recently failed fast attack craft rudder and existing rudder fabrication process in order to minimize this type of rudder failures in future. Analysis of failed rudder and the existing rudder fabrication process was done through macro/micro level inspection, chemical composition analysis and micro hardness testing of relevant materials.

Analysis revealed that rudder failed from the welded joint where rudder blade connected to rudderstock and weakening of the weld joint during fabrication. The weld joint was weakened due to formation of intermetallic phases, carbide precipitation, porosities and hot cracks in the heat affected zone of the weld. Therefore, finally rudder was failed as a result of fatigue failure. Use of similar low carbon stainless steel with suitable welding electrodes to ensure final weld lies in austenite region with containing 4% to 12% ferrite in the weld could overcome this issue.

Key words: Stainless steel, intermetallic phases, carbide precipitation.



University of Moratuwa, Sri Lanka.
Electronic Theses & Dissertations
www.lib.mrt.ac.lk

ACKNOWLEDGEMENT

I take this opportunity to forward my greatest gratitude to the University of Moratuwa, for letting me to do the postgraduate degree in Materials Science in the Department of Materials Science and Engineering.

I would like to express my heartfelt gratitude to the supervisor of my research, senior lecturer of the Department of Materials Science and Engineering, Eng. S.P Guluwita, for his understanding, guidance, enthusiasm and encouragement to complete this research. I would like to express my sincere thanks to the senior lecturers of the Department of Materials Science and Engineering, Dr. Shantha Amarasinghe and Mr. V. Shivar for their valuable advices and guidance given throughout this study. Also I would like to thank all the members of academic staff of Department of Materials Science & Engineering for their comments to improve the quality of this research.



University of Moratuwa, Sri Lanka.

I am extremely grateful to my employer, Sri Lanka Navy, for offering me the sponsorship for the degree Master of Science in Materials Science. I would like to thank all engineering staff of the Naval Dockyard, Trincomalee, for allowing me to use the facilities of the workshops. Also I am thankful to the non academic staff of Materials Science Laboratory at the University of Moratuwa, for their help given in many ways. Further, I wish to thank Technical Assistant, Mr. K.A. Sanjeewa of Industrial Technological Institute, for supporting me to get the chemical composition analysis of relevant metals.

Last but not least, I am fully indebted to my wife, for taking care of the family while I am busy with the research work.

TABLE OF CONTENT	Page No.
Declaration	i
Abstract	ii
Acknowledgement	iii
Table of content	iv
List of figures	vi
List of tables	viii
List of abbreviations	ix
1. Introduction	1
2. Literature survey	3
2.1 Rudder materials	3
2.1.1 Effect of alloying	6
2.1.2 Alloy steels	8
2.1.3 Role of alloying elements	10
2.2 Welding of stainless steel	12
2.2.1 Carbide precipitation	12
2.2.2 Hot cracking	14
2.2.3 Distortion and warpage	15
2.2.4 Porosities in the weld	16
2.3 Fatigue strength	16
2.4 Corrosion fatigue	17
2.5 Corrosion on stainless steel	17
2.5.1 Pittings and Crevice corrosion	18
2.5.2 Intergranular corrosion	18
2.5.3 Stress corrosion cracking	18
2.6 Back ground of similar rudder failures in other countries	19
2.6.1 Case 1	19
2.6.2 Case 2	20
2.6.3 Case 3	20

3. Methodology	22
3.1 Material used	22
3.2 Apparatus used	22
3.3 Experimental work	23
3.3.1 Examination of failed rudder	23
3.3.2 Examination of existing rudder fabrication process	26
4. Results and Discussion	29
4.1 Analysis of failed rudder	29
4.1.1 Macro level inspection	29
4.1.2 Microstructure analysis	31
4.1.3 Chemical composition analysis	34
4.1.4 Micro hardness testing	37
4.2 Analysis of existing rudder fabrication process	40
4.2.1 Selection of materials	40
4.2.2 Welding process	40
4.2.3 Chemical composition analysis	42
4.2.4 Microstructure analysis	44
4.2.5 Micro hardness testing	44
4.3 Calculation of cross sectional area of weld fill	47
5. Conclusion	48
6. Recommendations	49
References	50



List of Figures

Figure 1.1 :	Conventional propulsion ship	1
Figure 1.2 :	Arrangement of a rudder	1
Figure 2.1 :	Iron-iron carbide equilibrium phase diagram	3
Figure 2.2 :	Austenite to pearlite transformation on TTT diagram	5
Figure 2.3 :	Hardness vs different sizes of pearlite	5
Figure 2.4 :	Schaeffler Delong diagram	8
Figure 2.5 :	Sensitization	13
Figure 2.6 :	Carbide precipitation and chromium depletion	13
Figure 2.7 :	Hot cracking	14
Figure 2.8 :	Weld design of 'U' groove	15
Figure 2.9 :	Weld design of 'V' groove	15
Figure 2.10 :	Porosity	16
Figure 2.11 :	Failed rudderstock of Tanker ship	19
Figure 2.12 :	Failed rudderstock of Lightwave 485 sailing boat	20
Figure 2.13 :	Failed rudderstock of Catamaran hull sailing boat	21
Figure 3.1 :	Failed rudder stock	23
Figure 3.2 :	Specimen extracted sequence from failed rudder	24
Figure 3.3 :	Selected materials to fabricate a rudder	26
Figure 4.1 :	Photograph to show pattern of fracture surface	29
Figure 4.2 :	Microscopic picture taken to show crack initiation	30
Figure 4.3 :	Welding joint of inner shaft to outer rudder blade	30
Figure 4.4 :	Defects on failed rudder specimen	31
Figure 4.5 :	Specimen of failed rudder	31
Figure 4.6 :	Microstructure of all sections of specimen	32
Figure 4.7 :	Microstructure of metal A	32

Figure 4.8 :	Microstructure of HAZ ₁ between metal A and weld (B)	33
Figure 4.9 :	Microstructure of weld (B)	33
Figure 4.10 :	Microstructure of HAZ ₂ between weld (B) and metal C	33
Figure 4.11 :	Microstructure of metal C	34
Figure 4.12:	Failed rudder metals plot on Schaeffler Delong diagram	36
Figure 4.13 :	Graph of micro hardness vs distance(failed rudder)	38
Figure 4.14 :	Arrangement of shafts prior welding	40
Figure 4.15 :	Porosities in sample weld piece	41
Figure 4.16 :	Schaeffler Delong diagram for new rudder metals	43
Figure 4.17 :	Microstructure of HAZ of used shaft	44
Figure 4.18 :	Sample weld piece	44
Figure 4.19 :	Graph of micro hardness vs distance	46



University of Moratuwa, Sri Lanka.
Electronic Theses & Dissertations
www.lib.mrt.ac.lk

List of Tables

Table 2.1 :	Properties of different phases of iron	4
Table 4.1 :	Chemical composition of failed rudder material	35
Table 4.2 :	Micro hardness values of the sample(failed rudder)	38
Table 4.3 :	Chemical composition readings of new rudder metals	42
Table 4.4 :	Micro hardness values of the sample	45



University of Moratuwa, Sri Lanka.
Electronic Theses & Dissertations
www.lib.mrt.ac.lk

List of Abbreviations

Abbreviation		Description
BCC	-	Body Centered Cubic
FAC	-	Fast Attack Craft
FCC	-	Face Centered Cubic
FN	-	Ferrite Number
HAZ	-	Heat Affected Zone
ITI	-	Industrial Technological Institute
TTT	-	Time Temperature Transformation



University of Moratuwa, Sri Lanka.
Electronic Theses & Dissertations
www.lib.mrt.ac.lk

1. INTRODUCTION

Sri Lanka Navy's Fast Attack Craft(FAC) squadron consists of different types of craft which were built at various countries. Out of these craft, there are 12 Nos of Israel made fast attack craft which are equipped with conventional propulsion system. Rudders of these craft are used for maneuvering the craft at sea and it is very difficult to maneuver them without a rudder. Figure 1.1 shows the arrangement of a craft equipped with conventional propulsion system.

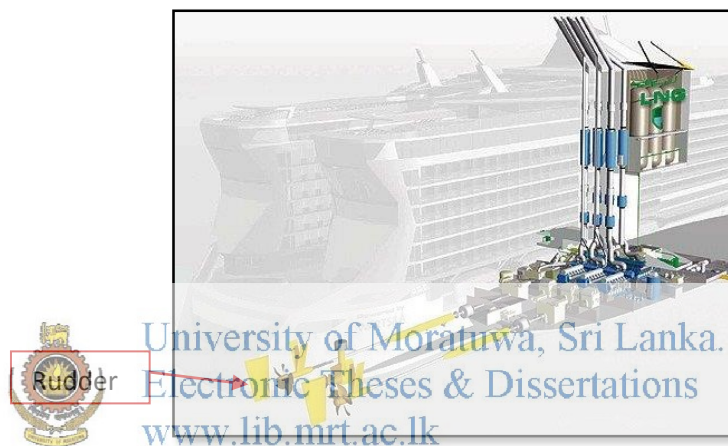


Figure 1.1 : Conventional propulsion ship

Rudders of these craft were made of stainless steel material and arrangement of a rudder is shown in figure 1.2.

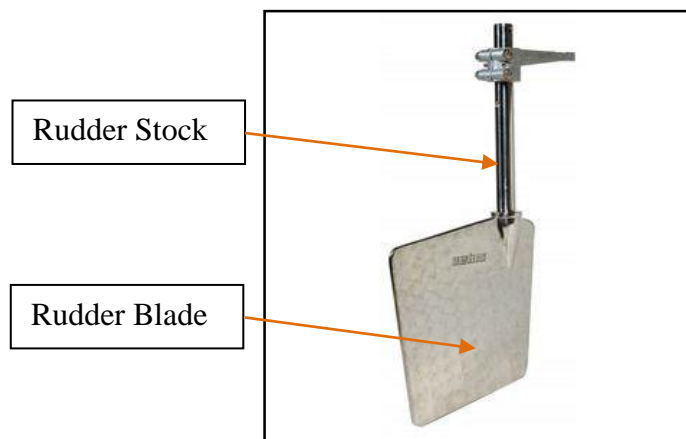


Figure 1.2 : Arrangement of a rudder

However, during the last few years, it was observed that frequent rudder failures of these craft and most of failures occurred from the place where rudder blade connected to its stock.

These failures were caused to become craft non operational and unavailable for several months. Since, there were neither local nor foreign suppliers to provide original rudders and non availability of local possible/reasonable fabricators, in-house fabricated rudders was used. However, these in-house fabricated rudders also were failed. Therefore, it was unable to effectively utilize these craft for operational requirements in the Navy.

The main objectives of this research are to analyze a fast attack craft rudder failure and to findout deficiencies of existing rudder fabrication process in order to minimize this type of rudder failures in future.



University of Moratuwa, Sri Lanka.
Electronic Theses & Dissertations
www.lib.mrt.ac.lk

2. LITERATURE SURVEY

This chapter includes brief description of materials, stainless steel types, behavior of material and changes of material properties during welding process and various welding defects. The research was done thereafter.

2.1 Rudder Materials

The performance and the durability of a rudder depend on its material properties. Further, material properties depend on its chemical composition and behavior of material during operation/design. As a first step on analyzing rudder material, Iron-Iron carbide equilibrium phase diagram, its phases present and change of their properties during heat treatment were considered. Figure 2.1 illustrate Iron-Iron carbide equilibrium phase diagram.

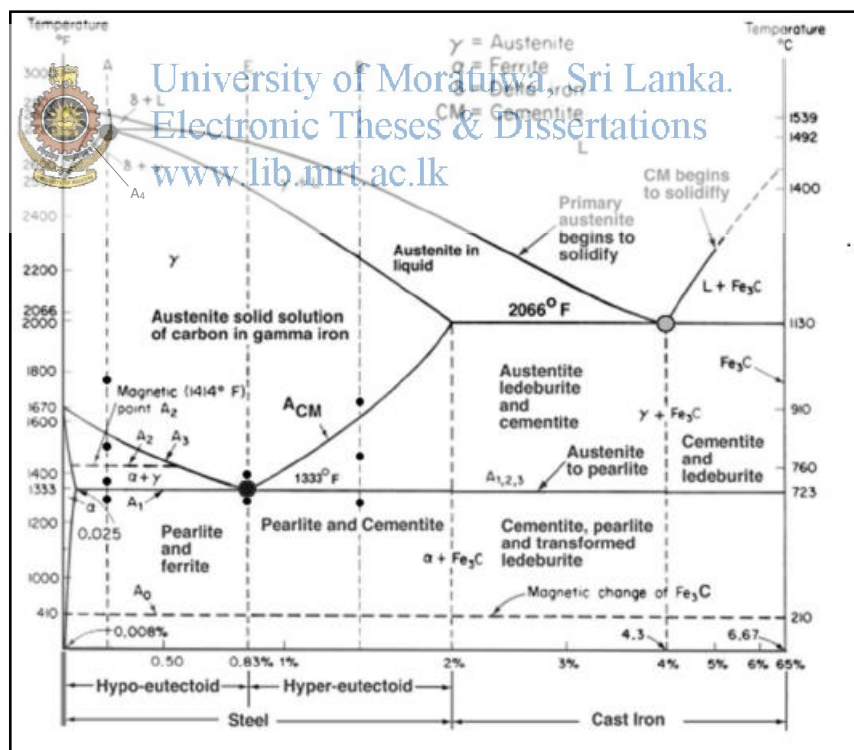


Figure 2.1 : Iron-Iron carbide equilibrium phase diagram[1]

Iron-Iron carbide equilibrium phase diagram depicts, pure iron, which upon heating, experiences two changes in crystal structure before it melts. At room temperature the stable form, call ferrite, or α -Iron, has a Body Centered Cubic (BCC) crystal structure. Ferrite experiences a polymorphic transformation to Face Centered Cubic (FCC) austenite, or γ -Iron, at 912°C (1674°F). This austenite persists to 1394°C (2541°F), at which temperature the FCC austenite revert back to a BCC phase known as δ -ferrite, which finally melts at 1538°C (2800°F) [2]. Properties of these phases are indicated in table 2.1.

Table 2.1: Properties of different phases of iron [3]

Ferrite(α)-Iron	Austenite(γ)-Iron	Delta(δ)-Iron
BCC Structure	FCC Structure	BCC Structure
Ferromagnetic	Non-magnetic	Paramagnetic
Carbon solubility low, up to 0.022 wt % C	Carbon solubility up to 2.14 wt % C	Carbon solubility low

Phase transformations are important in the processing of materials, and usually involve some alteration of the microstructure. With phase transformation, normally at least one new phase is forming that has different physical/chemical characteristics and/or a different structure than the parent phase [3].

Phase transformation commonly occurs by the processes of nucleation and grain growth. Therefore, time taken for a transformation to go to completion is important in the control of the structure of a material. The time taken depends on the nature and the mechanism by which a phase transformation is brought about. Further, based on transformation temperature also microstructure and its physical properties of a material will change [4]. Microstructures of Austenite to Pearlite transformation on Time Temperature Transformation (TTT) diagram for a 1080 Eutectoid Steel is shown in figure 2.2.

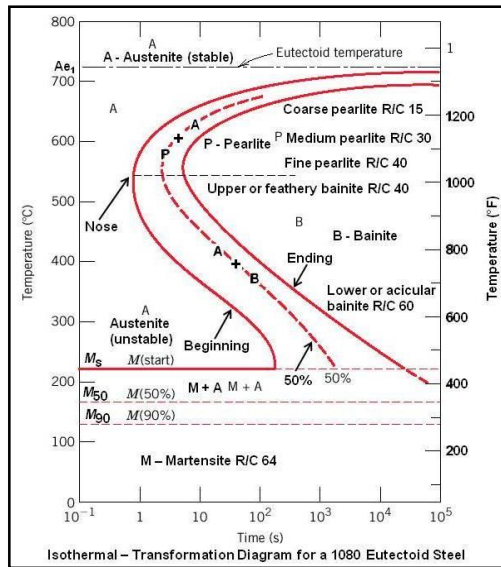


Figure 2.2 : Austenite to Pearlite transformation on TTT diagram [5]

The absolute layer thickness depends on the temperature of the transformation. At higher temperature, nucleation is slow and diffusion is fast, few nuclei are formed but the cementite plates grow rapidly, this results to form coarse pearlite of relatively thick platelets. At lower temperatures, where nucleation is fast but growing is slow, one obtains a fine pearlite formed of closely spaced fine platelets of ferrite and cementite [6]. Hardness of different pearlites is shown in figure 2.3.

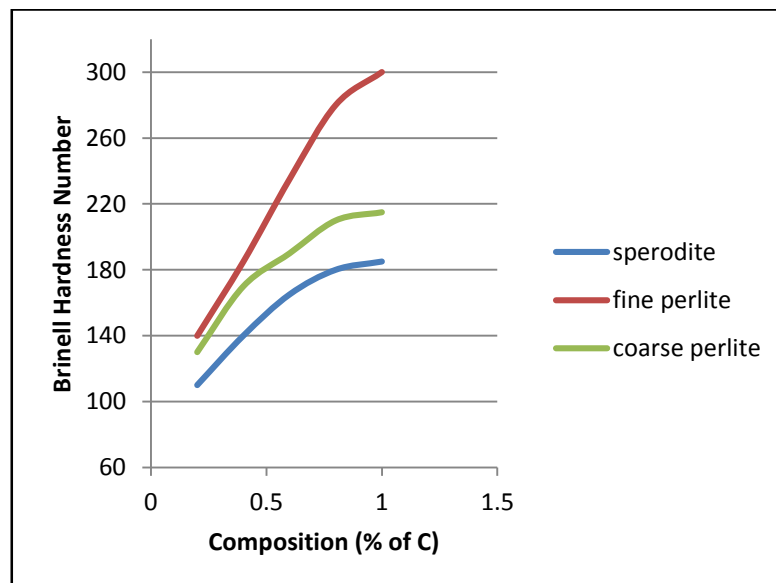


Figure 2.3 : Hardness vs different sizes of pearlite

There do exist mainly two types of steels which are plain carbon steel and alloy steel. Plain carbon steels do have some appreciable properties but also consists of some limitations such as [7].

- a. Poor hardenability.
- b. Enhanced strength at the cost of toughness and ductility.
- c. Poor resistance to softening during tempering.
- d. Inadequate elevated temperature properties.
- e. Insufficient resistance to corrosion and oxidation.
- f. Susceptibility to grain growth, decarburization and soft spots.

Therefore, alloying elements like Cr, Ni, Mn, Mo, Nb, Ti, W, Co, Cu, V, Si, Al, B, N, Pb and Ca are added to steel with the objective of improve existing properties and introduce new properties which are not available on plain carbon steel.

2.1.1 Effects of Alloying

2.1.1.1 Polymorphic Transformation Temperatures



University of Moratuwa, Sri Lanka.
Electronic Theses & Dissertations

In Iron-Iron-carbide phase diagram (figure 2.1), A_3 temperature where ferrite(α) to austenite(γ) transformation and A_4 temperature where austenite(γ) to Delta(δ) iron transformation take place. Some elements like Ni, Mn, Co and Cu raise A_4 temperature and lower A_3 temperature thus increases austenite phase. They are called austenite stabilizers. Other elements like Cr, W, V, Mo, Al and Si raise A_3 and lower A_4 thus widen ferrite phase. They are called ferrite stabilizers [1].

2.1.1.2 Formation and Stability of Carbides

Some alloying elements form hard carbides to provide greater wear resistance. Alloying elements that are strong carbide formers, such as titanium or vanadium, help in preventing grain growth at elevated temperatures by pinning the grain boundaries [8].

2.1.1.3 Effect of Grain Growth

Presence of Chromium, result in an increased rate of grain growth in steel. In the case of overheating the steel, it can promote brittleness which is the usual outcome with coarse grain. Grain growth retarded by elements like V, Ti, Nb, Al and Ni. V is probably the best for grain refining [9].

2.1.1.4 Effect of Displacement of Eutectoid Point

Adding of alloying elements to steels reduces the solubility of carbon in Austenite thus results in displacement of eutectoid point to the left [10].

2.1.1.5 Retardation of Transformation Rates

Alloying elements such as Mn, Ni, Cr, V, W and Mo, have the effect of shifting the nose of the C curve of TTT diagram to the right. This enables forming martensite at slow cooling rates and without cracking the steel [4].

2.1.1.6



University of Moratuwa, Sri Lanka.
Electronic Theses & Dissertations
www.lib.mrt.ac.lk

Effects on Corrosion Resistance

Corrosion resistance of steel is increased by adding Cr, Si and Al. this is due to the formation of thin dense and adherent chromium oxide film on the surface of steel [6].

2.1.1.7 Effect on Mechanical Properties

The most important reason for adding alloying element to steel is to increase hardenability. The most effective alloying elements for increasing hardenability are manganese, chromium, molybdenum and nickel. Generally, higher alloy content, the greater the hardenability and higher the carbon content, the greater the strength [8].

Since there are various effects on steel after adding of alloying elements, it is very important to know about the combine effect in order to construct alloy steels for particular application. Schaeffler Delong diagram at figure 2.4 depicts phases present in alloys as-solidified condition, such as found in the weld [11].

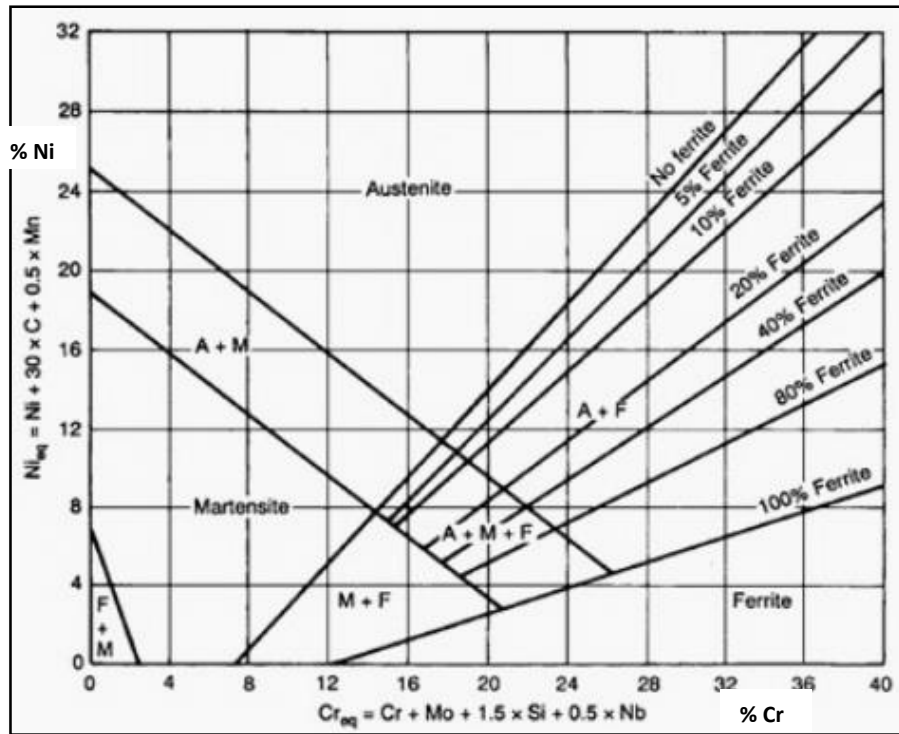


Figure 2.4 : Schaeffler Delong diagram [11]

2.1.2 Alloy Steels



University of Moratuwa, Sri Lanka.
Electronic Theses & Dissertations
www.lib.mrt.ac.lk

Alloy steels are broadly classified into two groups as low alloy steels having alloy content less than 10% by wt. and high alloy steels having alloy content more than 10% by wt. [12]. Stainless steels are iron-based alloys containing at least 10.5% Cr, which are used primarily for their corrosion resistance. There are many different stainless steels, but they all meet this minimum chromium requirement [13]. Mainly four sub groups of stainless steels are available and they are as follows [14];

- a. Ferritic stainless steel.
- b. Martensitic and Precipitation hardened stainless steel.
- c. Austenitic stainless steel.
- d. Duplex stainless steel.

2.1.2.1 Ferritic Stainless Steel (FSS)

Ferritic stainless steels contain 12-30%Cr with relatively low amount of C. Structure is ferritic at room temperature and not hardenable by heat treatment as structure remains as ferrite until melting point. These steel includes AISI types 405, 409, 430, 436, 446 etc. [2]. This type of steels are magnetic, have good ductility and resistance to corrosion/oxidation. Grain refinement by phase transformation not possible due to ferrite structure remains until melting point. Cold work and recrystallization can refine grains [14].

2.1.2.2 Martensitic and Precipitation Hardened Stainless Steel

These stainless steels contain 12-18%Cr with sufficient C and room temperature microstructure is martensite. These steels will transform to austenite on heating and, therefore, can be hardened by formation of martensite on cooling. They have a tendency towards weld cracking on cooling when hard brittle martensite is formed [2]. These stainless steels are less corrosion resistance and cheaper than other types of stainless steels. These grades are magnetic. The fatigue properties of the martensitic stainless steel depend on heat treatment and design. A notch in a structure or the effect of a corrosive environment can do more to reduce fatigue limit than alloy content or heat treatment [15].

2.1.2.3 Austenitic Stainless Steel (ASS)

Austenitic stainless steel contains 16-25%Cr and 8-22%Ni. Room temperature microstructure is austenite. Not hardenable by heat treatment as presence of only austenite phase. Since, austenite has FCC structure, can be easily cold formed and cold working hardens the material [16]. They have excellent corrosion resistance, usually good formability and increases strength as a result of cold work. Austenitic stainless steels are using most widely among other stainless steel types. But these types are susceptible to intergranular corrosion which can be overcome by lowering carbon content [15].

2.1.2.4 Duplex Stainless Steel

Duplex grades have ferritic and austenite microstructure, with the phase balance of approximately 50% ferrite and 50% austenite. Duplex grades combine many of the beneficial properties of ferrite and austenite stainless steel. The duplex microstructures also contribute to the high strength and high resistance to stress corrosion cracking. Duplex grades are magnetic due to the ferrite content [14].

2.1.3 Role of Alloying Element

Chemical composition has a major influence on steel's metallurgical structure, mechanical properties, physical properties and corrosion resistance. Choosing a particular composition often requires the designer or the material engineer to sacrifice a measure of one property to maximize the benefit of other [13]. Functions of some important alloying elements are as follows.

2.1.3.1 Chromium (Cr)

Chromium is the alloying element that imparts to stainless steels their corrosion resistance qualities by combining with oxygen to form a thin, invisible chromium oxide protective film on the steel surface [15]. It provides corrosion resistance and resistance to oxidation at high temperature. Chromium is a ferrite former [14].

2.1.3.2 Nickel (Ni)

Nickel's primary purpose is to create and stabilize austenite [4]. Nickel increases toughness and impact resistance, good properties at low temperatures. With other alloys imparts excellent corrosion resistance. Nickel increases strength with little loss of ductility [10].

2.1.3.3 Carbon (C)

Carbon is a strong austenite former that also significantly increases the mechanical strength. However, it reduces the resistance to intergranular corrosion, caused by carbide formation. In ferritic steels carbon reduces the toughness and corrosion

resistance. In martensite steel carbon increases the hardness and strength, but reduces the toughness [14].

2.1.3.4 Molybdenum (Mo)

Molybdenum significantly reduces the both uniform and localized corrosion. It is a strong ferrite former and increases the mechanical strength. Molybdenum enhances the risk for the formation of secondary phases in ferrite, duplex and austenite steels. In martensitic steels it increases the hardness at higher tempering temperatures due to its effect on the carbide precipitation [14].

2.1.3.5 Manganese (Mn)

Manganese is used in stainless steel to increase ductility and hardenability. Manganese also have high strain hardening capacity and enhance wear resistance [10].

2.1.3.6 Silicon (Si)

Silicon is a deoxidizer and promotes graphite precipitations, it also increases the strength and wear resistance of steel while significantly increasing the elastic limit [17].

2.1.3.7 Titanium (Ti) , Niobium (Nb)

Titanium is strong carbide former and a strong ferrite former. It increases the resistance to intergranular corrosion by forming of carbides and also increases mechanical properties at high temperature [13].

2.1.3.8 Nitrogen (N)

Nitrogen is a very strong austenite former that also significantly increases the mechanical strength. In ferritic stainless steel nitrogen will strongly reduce toughness and corrosion resistance. In martensitic steel nitrogen increases both hardness and strength but reduces toughness [14].

2.2 Welding of Stainless Steel

Since austenitic type stainless steels were used for rudder construction, Austenitic stainless steel welding was considered under this topic. Austenitic stainless steels have lower coefficient of thermal conductivity, which causes a tendency for heat to concentrate in a small zone adjacent to the weld [16]. Further, less welding heat input is required to make a weld because the heat is not conducted away from the joint as rapidly as in carbon steel. These steel also have coefficient of thermal expansion approximately 50% greater than carbon steel, which require more attention to control warpage and distortion [2]. Therefore, successful performance of the welding of austenitic stainless steel requires proper selection of alloys for both base metal and filling metals and use of correct welding procedures [18].

Following problems are associated with the welding of austenitic stainless steels and suitable/correct welding processes are to be applied to prevent these defects [16].

- a. Carbide precipitation.
- b. Hot cracking.
- c. Distortions and warping.
- d. Porosities in the weld.

2.2.1 Carbide Precipitation

During the welding at high temperature chromium combines with available carbon in the vicinity of grain boundaries and form chromium carbides. Formation of these chromium carbides and precipitation at grain boundaries in the heat affected zone, causes to produce area depletion in chromium. The region immediately next to the chromium carbide particle is denuded of chromium and, therefore, becomes anodic to the interior of the grain. A galvanic cell is set up and corrosion occurs close to the grain boundaries. This is called intergranular corrosion [4]. The carbide formation depends on following factors [2] and same illustrated at figure 2.5.

- a. The metal temperature range between 425⁰C to 900⁰C. Chromium carbide form more rapidly at 650⁰C temperature.

b. Percentage of carbon content in the material. Carbide formation increases with high carbon content.

c. Time at temperature. Few seconds at 650°C temperature causes to form more Chromium carbides.

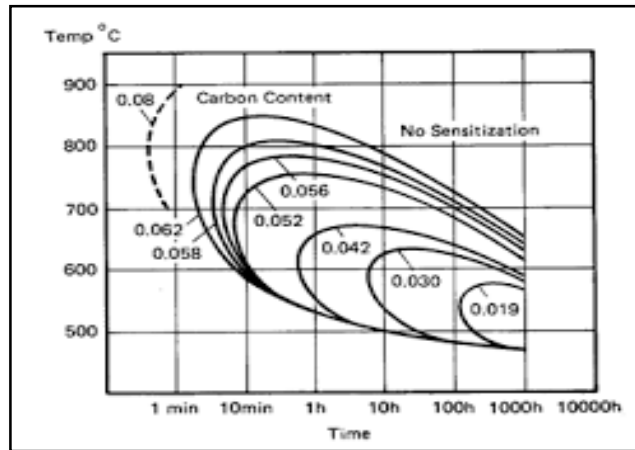


Figure 2.5 : Sensitization [19]

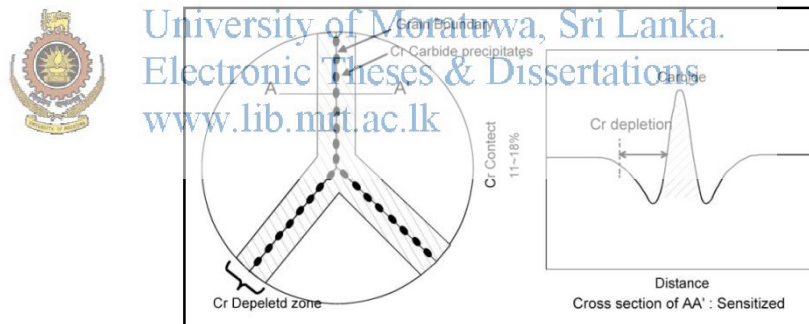


Figure 2.6 : Carbide precipitation and chromium depletion zones [20]

Figure 2.6 shows that the local chromium depletion is such that the chromium level can become low enough that it is not even enough to be stainless and certainly will have much low corrosion resistance than the surrounding area [11]. Carbide precipitation could be controlled by following means [16].

a. Use of low carbon base metal and filling metals. Extra low carbon grade stainless steels such as 304L and 308L which are having carbon content of 0.04% are most often used for weldments which operate in severe corrosive environments.

b. Use of stabilized grades containing small amount of Titanium, Niobium or combination of Titanium and Niobium. These elements are strong carbide formers than chromium, thus leaving chromium to provide corrosion resistance.

c. Amount of carbide precipitation could be reduced by promoting rapid cooling. Use of copper chill bars, skip welding and other techniques help to reduce carbide precipitation.

2.2.2 Hot Cracking

Hot cracking is caused by low melting materials such as metallic compounds of sulfur and phosphorous which tends to penetrate grain boundaries. When these compounds are present in the weld or heat affected zone, they will penetrate grain boundaries and cracks will appear as weld cools and shrinkage stresses developed. Hot cracking increases remarkably for phosphorus and sulfur contents in excess of 0.015% and 0.010% respectively [21]. Hot cracking can be prevented by adjusting the composition of the base materials and filler materials to obtain a microstructure with a small amount of ferrite in the austenite matrix. The ferrite provides ferrite-austenite grain boundaries which are able to control the sulfur and phosphorous compounds so they do not permit hot cracking. It is essential to use filler metal that can create 5% to 10% ferrite in the welded microstructure, which is required to prevent solidification cracking [22]. The ferrite content at the weld metal and the heat affected zone should be in the range of 25% - 75% to give optimum mechanical properties and corrosion resistance[23]. Figure 2.7 shows a hot crack at the weld.



Figure 2.7 : Hot Cracking [24]

2.2.3 Distortion and Warpage

Since the coefficient of thermal expansion for austenitic stainless steel is relatively high, the control of distortion must be considered in designing weldments. The volume of weld metal in joints must be limited to the smallest size which will provide the necessary properties. It was calculated and proved that, in thick plates, a 'U' groove (figure 2.8), which gives a smaller volume than a 'V' groove (figure 2.9). This not only reduces the volume of the weld metal required but also helps to balance the shrinkage stresses. Relevant calculations of cross sectional area of weld fill which was done for both 'U' and 'V' groove one half (section x) indicated at section 4.3.

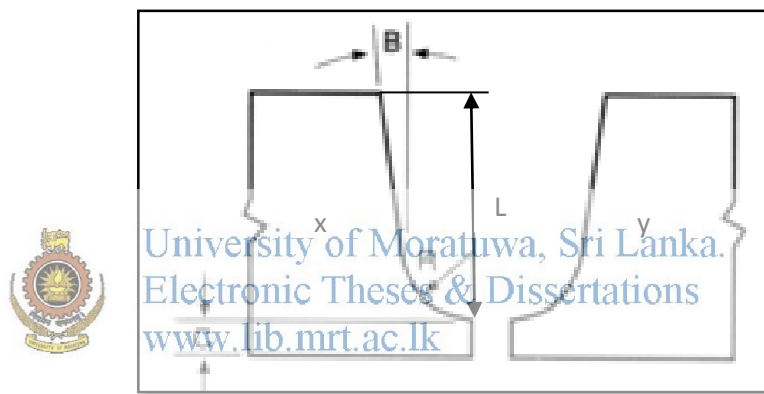


Figure 2.8 : Weld design of 'U' groove [26]

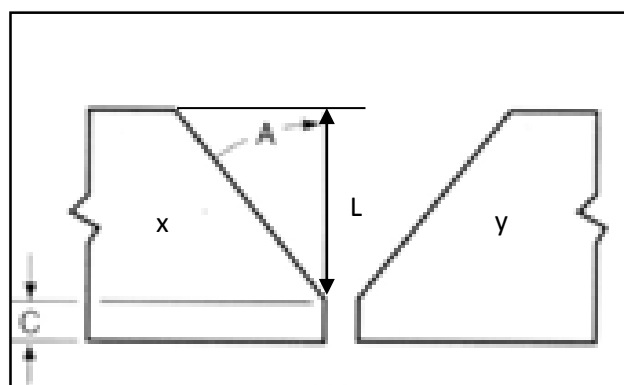


Figure 2.9 : Weld design of 'V' groove [26]

Accurate joint fit up and careful joint preparations which are necessary for high quality welds also help minimize distortion. Joint location and weld sequence should be considered to minimize distortion. Strong tooling and fixturing should be employed to hold parts in place and resists tendencies for component to move during welding [2]. Further, low welding current with high travel speed is preferable to minimize this defect [25].

2.2.4 Porosities in the Weld

Hydrogen can be a cause of blowholes and porosity in stainless steels. The residual hydrogen content of stainless steel is within safe limits, so the problem occurs when this residual hydrogen is supplemented by other sources often deceptive. A few examples of deceptive sources of unwanted hydrogen are damp fluxes, weld rod coatings, improperly compounded electrode coverings and imperfectly sealed joints in welding torch cooling systems which bleed water vapour [16]. Microstructure of the cross section of the sample containing high porosity is shown in figure 2.10.

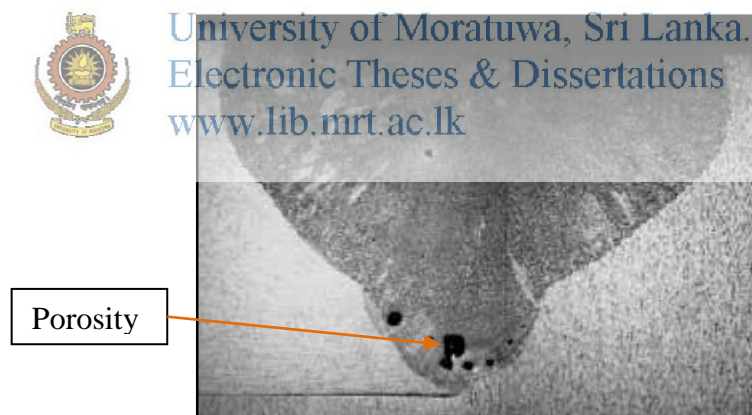


Figure 2.10 : Porosity [27]

2.3 Fatigue Strength

Fatigue is the progressive and localized structural damage that occurs when a material is subjected to cyclic loading. Microscopic cracks will begin to form if the loads are above a certain threshold. Eventually a crack will reach a critical size and

the structure will suddenly fracture due to rapid crack propagation. The shape of the structure will significantly affect the fatigue life. Welds, square holes and sharp corners will lead to elevated local stresses where a fatigue crack can initiate. Therefore, round holes and smooth transitions are important to increase the fatigue strength of a structure [16]. Welded joints are subjected to various forms of cyclic loadings in practical applications and fatigue failure is common. Thus, welding is a major factor in the fatigue lifetime reduction of components [28].

2.4 Corrosion Fatigue

If the material is simultaneously exposed to a corrosive environment, failure may occur at even lower load levels and after shorter period of time. This failure by a combination of cyclic load and corrosive environment is called corrosion fatigue [29].

The more aggressive corrosive conditions and lower the loading frequency the higher the effect of environment. At lower frequencies, the corrosive action is more pronounced and an aggressive environment may also cause corrosion attack that can act as a stress concentrator and thus contribute to a shorter life. Increasing mechanical strength of stainless steel also increases their resistance to corrosion fatigue [29].

2.5 Corrosion on Stainless Steel

Corrosion resistance of stainless steel is achieved by forming of passive film of iron and chloride oxides or hydroxides with the thickness of 1-3nm on the surface of stainless steel. As the passive film adheres strongly to the metal surface and protect it from contact with the surrounding environment, the electrochemical reactions causing corrosion are brought to a halt [29].

All corrosion types affecting stainless steel are related to permanent damage of the passive film, either complete or local breakdown. Factors such as chemical environment, PH, temperature, surface finish, product design, fabrication method,

contaminations and maintenance procedures will all affect the corrosion behavior of stainless steel and the type of corrosion that may occur [29].

2.5.1 Pitting and Crevice Corrosion

Stainless steels are particularly susceptible to pitting and crevice corrosion in media containing halide ions such as chloride. Therefore, environments that represent a risk for pitting and crevice corrosion include seawater and process solutions containing high concentrations of chlorides. Once these corruptions initiate they propagate very fast [29].

2.5.2 Intergranular Corrosion

Intergranular corrosion is the preferential corrosion of the grain boundary regions that can occur as a consequence of the precipitation of chromium carbides and intermetallic phases. In the presence of large quantities of Cr and Mo, intermetallic phases such as brittle tetragonal sigma phases are formed [30]. Creation of sigma phase is a chromium consumable reaction. Therefore, chromium-depleted zones surrounding sigma phase particles will be produced, which have the lowest corrosion resistance [31]. Susceptibility to intergranular corrosion is increased by the chromium depletion generated by the formation of chromium rich carbides at the grain boundaries (sensitization) which occurs readily in the temperature range of 500^o – 900^o C [32]. In a corrosive environment the chromium depleted areas may be attacked and the unfavorable anode to cathode surface area ratio accelerates the attack along the grain boundaries. A small amount of delta-ferrite in austenitic stainless steels also improves the resistance to intergranular corrosion as carbides precipitate at austenite-ferrite phase boundaries rather than at the austenitic grain boundaries [33].

2.5.3 Stress Corrosion Cracking

Like pitting and crevice corrosion, stress corrosion cracking (SCC) most frequently occurs in chloride containing environments and alkali solutions. Elevated temperatures (> 60^oC) are normally required for SCC to occur in stainless steel. A

common cause of SCC is evaporation on hot stainless steel surfaces. SCC occurs across the grains. Stress corrosion crack propagating in the HAZ towards the fusion boundary(FB), showed slower growth after it reached the FB, primarily due to the change in the direction of the intergranular propagation [34]. Standard austenitic grades are generally sensitive to chloride induced stress corrosion cracking. High content of nickel and molibnium increases resistance to SCC of austenitic stainless steels.

2.6 Back Ground of Similar Rudder Failures in Other Countries

2.6.1 Case 1

Broken rudderstock due to corrosion fatigue of a Netherland Tanker ship in the year 2000[35].

While the Tanker sailing at sea, the steering gear failed to respond. Investigation revealed that the rudder was not in the position as indicated by the rudder angle indicator on the bridge and in the steering gear room.

Underwater inspection in dry dock revealed that the rudderstock was found broken, having sheared off where the rudder is secured to the rudderstock. After dismantling, the sheared surface at the break of the rudderstock indicated a typical fatigue failure. A picture of relevant broken rudderstock is shown in figure 2.11.

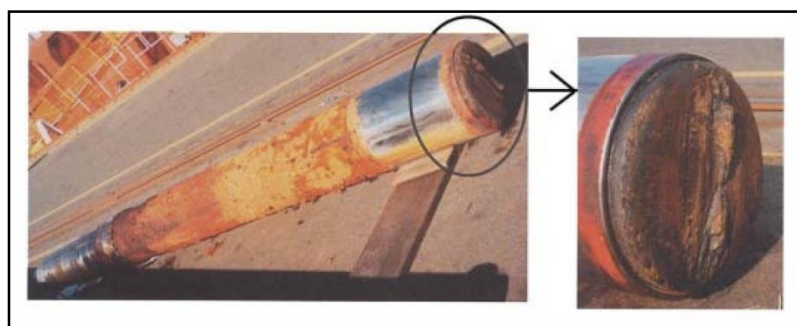


Figure 2.11: Failed rudderstock of Tanker ship [35]

2.6.2 Case 2

Rudder failure of lightwave 485 sailing boat during Rolex Middle Sea Race in the year 2015 [36].

While the sailing boat at the Rolex Middle Sea Race, experienced loss of boat control. Investigation revealed that broken of rudder from its rudderstock. The failure on the rudderstock happened at a welded joint inside the blade and relevant picture is shown in figure 2.12.



University of Moratuwa, Sri Lanka.

Figure 2.12: Failed rudderstock of lightwave 485 sailing boat [36]

Electronic Theses & Dissertations
www.lib.mrt.ac.lk

2.6.3 Case 3

Lost of starboard rudder of a Catamaran hull sailing boat near Tonga Island in the year 2014 [37].

While a Catamaran hull sailing boat sailing near Tonga Island, observed poor maneuverability of the boat and observe starboard rudder was not visible. Underwater inspection revealed that rudder broken from its rudderstock and break in the rudderstock was due to crevice corrosion. Relevant picture of the failed rudderstock is shown in figure 2.13.



Figure 2.13 : Failed rudderstock of Catamaran hull sailing boat [37]



University of Moratuwa, Sri Lanka.
Electronic Theses & Dissertations
www.lib.mrt.ac.lk

3. METHODOLOGY

3.1 Material Used

Different stainless steel grades were used for rudder fabrication and same was illustrated in subsequent sections.

3.2 Apparatus Used

The following apparatus were used in this research.

- | | | | |
|----|---------------------------|---|---|
| a. | Universal Lathe Machine | - | Center Lathe
Model : AJ 260 VS
Made in England |
| b. | Universal Shaping Machine | - | Model : HTANK
Made in USSR |
| c. | Power saw | - | Model : AJHD 250
Made in England |
| d. | Heat Tracer Gun | - | Make : Extech
Extech Instrument cooperation
USA |
| e. | Optical Microscope | - | Metallurgical Microscope
Olympus, Japan |
| f. | Micro hardness tester | - | Hardness Tester
Model : MMT-7
Matsuzawa Co-Ltd, Japan |
| g. | Universal Polisher | - | BUEHLER, USA |
| h. | Hand grinder | - | BUEHLER, USA |
| i. | Universal grinder | - | BUEHLER, USA |

3.3 Experimental Work

Experimental work was undertaken in two stages, viz.; the examination of failed rudder and examination of existing rudder fabrication process.

3.3.1 Examination of Failed Rudder

Examination of failed rudder was performed based on available recently failed rudder stock shown at figure 3.1.



Figure 3.1 : Failed rudder stock

3.3.1.1 Macro Level Inspection

Digital photographs and microscopic pictures were taken on the fracture surface of the failed rudder stock for macro level inspection.

The results are given in **4.1.1**

3.3.1.2 Microstructure Analysis

An optical microscope available at the University of Moratuwa was used for the observation of the metallographic microstructure of materials used for fabrication of failed rudder and the weld. Specimen was extracted from the failed rudder stock and extracted sequence for preparing the specimen from the failed rudder is shown in

figure 3.2 and following processes were carried out to prepare the specimen. Further, optical microscopic inspection was carried out to examine materials of all sections of the specimen.

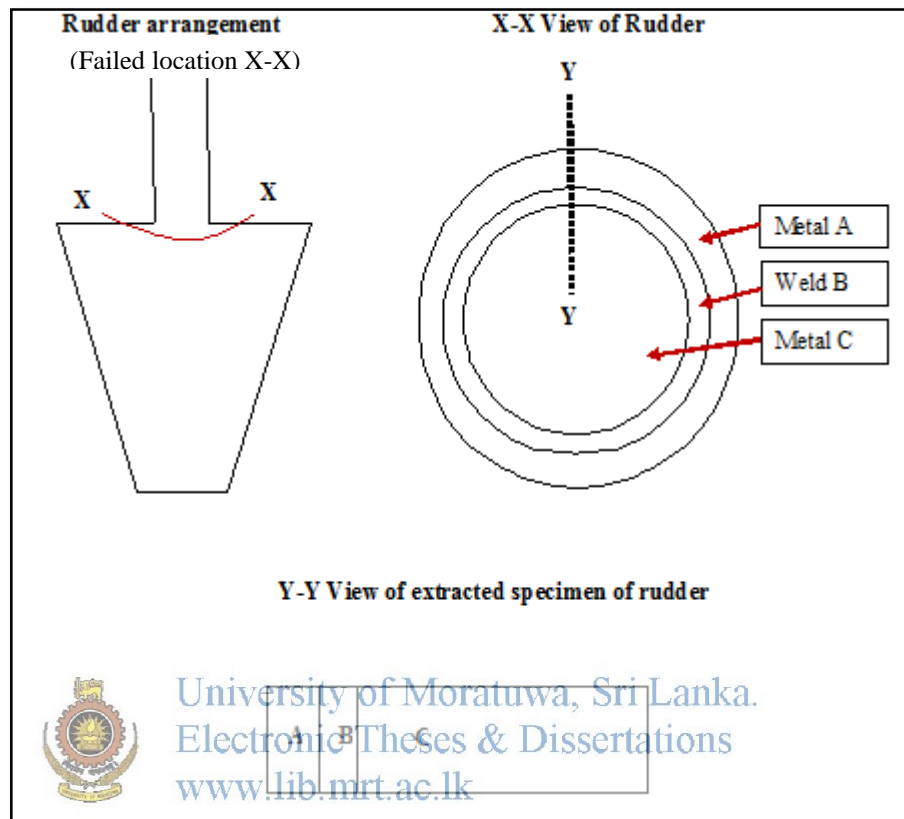


Figure 3.2 : Specimen extracted sequence from failed rudder

a. Cutting

Specimen was extracted by cutting of fracture surface area of the failed rudder (Y-Y section of figure 3.3) to get a specimen covering all three following sections as shown at figure 3.2.

- (1) A – Outer part (portion of rudder blade)
- (2) B – Weld area
- (3) C – Inner part (portion of rudder stock)

b. Grinding

Both hand grinder and Universal grinder were used to reduce the surface defects of the specimen to suitable level.

c. Polishing

Universal polishing machine was used to polish the specimen in order to clearly reveal the microstructure.

d. Etching

Chemical etching was done to inspect microstructure clearly. Initial etching was done using Ferric Chloride and Hydrochloric acid solution with compositions of ferric chloride (5g), Hydrochloric acid (50ml) and water (100ml). However, it was observed that outer part (A) of the specimen was not etched well with above etchant, hence, used Carpenter etchant which is having compositions of ferric chloride (8.5g), Cupric chloride (2.4g), Alcohol (122ml), Hydrochloric acid (122ml) and Nitric acid (6ml).



University of Moratuwa, Sri Lanka.
Electronic Theses & Dissertations

www.lib.mrt.ac.lk

The results are given in 4.1.2

3.3.1.3 Chemical Composition Analysis

Chemical composition analysis of failed rudder materials covering all sections was done using Atomic Absorption Spectroscopy which is available at Industrial Technological Institute.

The results are given in 4.1.3

3.3.1.4 Micro Hardness Testing

Micro hardness was also measured across weldment of failed rudder sample using the micro hardness tester available at the University of Moratuwa.

The results are given in 4.1.4

3.3.2 Examination of Existing Rudder Fabrication Process

In-house rudder fabrication was carried out at the Naval Dockyard, Trincomalee using the facilities available at the workshops. Processes involved during the rudder fabrication were monitored and laboratory tests were carried out for materials in order to analyze the process. Relevant processes are explained in following sections.

3.3.2.1 Selection of Materials

Used stainless steel propeller shafts which were removed from ships/craft due to exceeding of their wear limits were used to prepare rudder blade and procured stainless steel rod was used as rudder stock. A photograph of the selected shafts and rods is shown at figure 3.3.

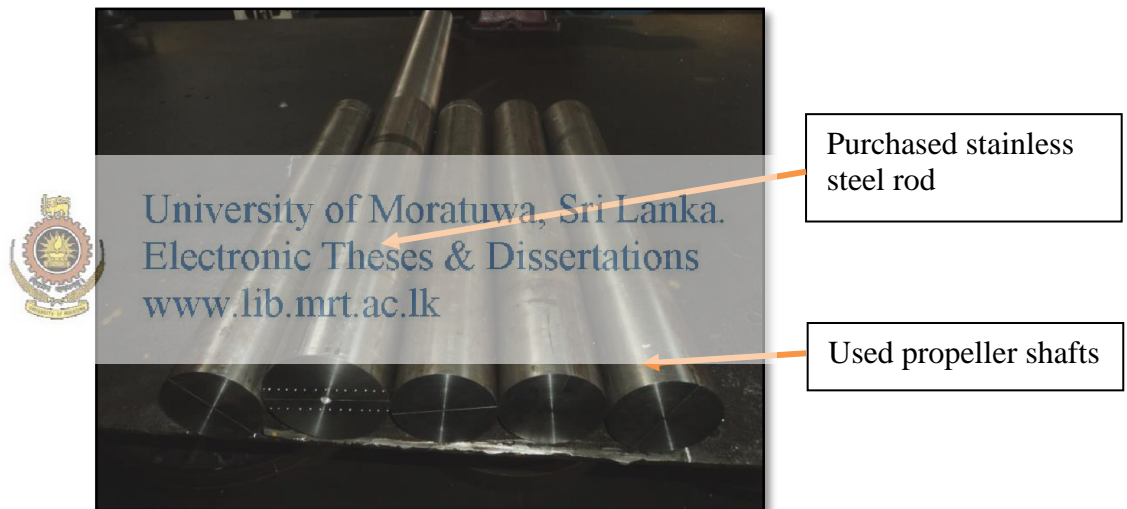


Figure 3.3 : Selected materials to fabricate a rudder

3.3.2.2 Mechanical Processes Involved

During the rudder fabrication following processes were performed and observed that temperature involvement during all these processes were negligible as proper cooling was provided during each process.

- a. Machining to get the required diameter using Universal Lathe machine.
- b. Cutting of shaft pieces to get the required lengths using power saw.

- c. Shaping of shafts to get the required dimensions as per original drawings using a shaping machine.

3.3.2.3 Monitoring of the Welding Process

The parameters of the welding process which were monitored are as follows.

- a. Welding rod used - Satincrome 316L-16
- b. Welding current - 75 – 100 A
- c. Continuous welding time - 45 – 60 second
- d. Welding type - Manual Arc
- e. Temperature involved - 1100 – 1400⁰F
- f. Cooling mode - Air cool
- g. Joint type of weld - Butt joint
- h. Groove type - Double V groove



Followings were also monitored which are related to the performance of stainless steel weld.

- a. As a general practice of welders, welding electrodes were kept at working place exposed to atmosphere till completion of the day’s work and place electrodes inside into hot cupboard. Some electrodes were kept in the hot cupboard for several weeks.
- b. Since the rudder blade requires smooth finish, grinding operations were performed heavily on the weld area using Aluminum carbide grinding discs. On completion of grinding, re-welding was carried out to fill void areas. This process was continued until getting required dimensions/finish.

c. As a general practice of welders, continued welding until completion of an entire welding electrode.

3.3.2.4 Chemical Composition Analysis

Chemical composition analysis of recently fabricated rudder materials was done using Atomic Absorption Spectroscopy which is available at ITI.

The results are given in **4.2.3**

3.3.2.5 Microstructure Analysis

The optical microscope available at the University of Moratuwa was used for the observation of the metallographic microstructure of the sample.

The results are given in **4.2.4**

3.3.2.6 Micro Hardness Testing

Micro hardness was measured across weldment of the sample weld piece using the micro hardness tester available at the University of Moratuwa.



University of Moratuwa
Electronic Theses & Dissertations
www.lib.mrt.ac.lk

The results are given in **4.2.5**

4. RESULTS AND DISCUSSION

Results and discussion based on the experimental work which was explained in the previous chapter are presented in this chapter.

4.1 Analysis of Failed Rudder

The results are discussed in the subsequent sections.

4.1.1 Macro Level Inspection

A digital photograph was taken to inspect the pattern of fracture surface which is shown at figure 4.1.

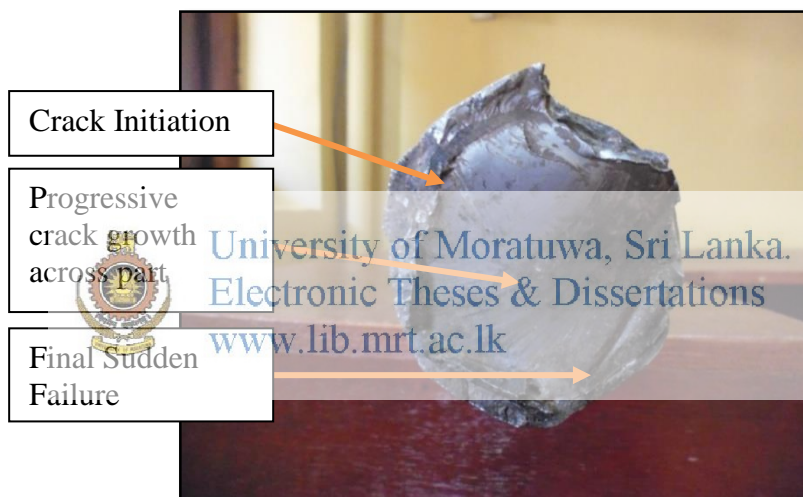


Figure 4.1 : Photograph to show pattern of fracture surface

Figure 4.1 was revealed that the pattern of fracture surface comprises all the three main sections of a fatigue failure. Crack initiation area, progressive crack growth across the part and the final sudden fracture sections are available on the fracture surface of failed rudder stock. Therefore, this rudder has failed as a result of fatigue. Further, a microscopic picture was taken to inspect internal crack area which is shown at figure 4.2 also was confirmed the initiation of crack.

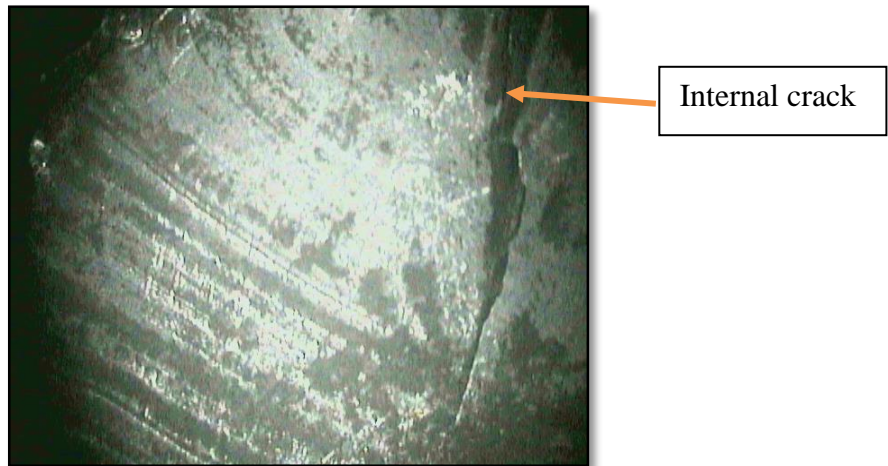


Figure 4.2 : Microscopic picture taken to show crack initiation on failed rudder

It was also observed that filling part of the weld joining inner shaft (rudder stock) to outer rudder blade portion looks completely different at the fracture surface and same is shown at figure 4.3.



Figure 4.3 : Welding joint of inner shaft to outer rudder blade portion

It was observed that there were number of defects in the weld such as considerable porosities and corrossions marks beside the weld. A specimen prepared from failed rudder stock shown at figure 4.4 revealed those defects.

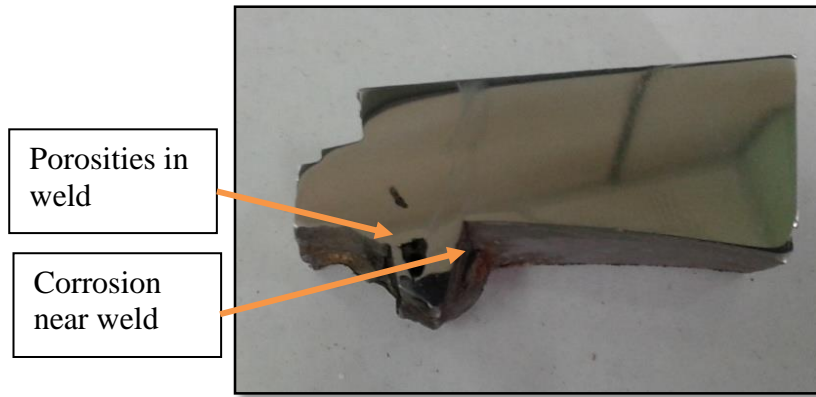


Figure 4.4 : Defects on failed rudder specimen

4.1.2 Microstructure Analysis

Microstructure of the specimen covering all three sections indicated at figure 4.5 is shown at figure 4.6.

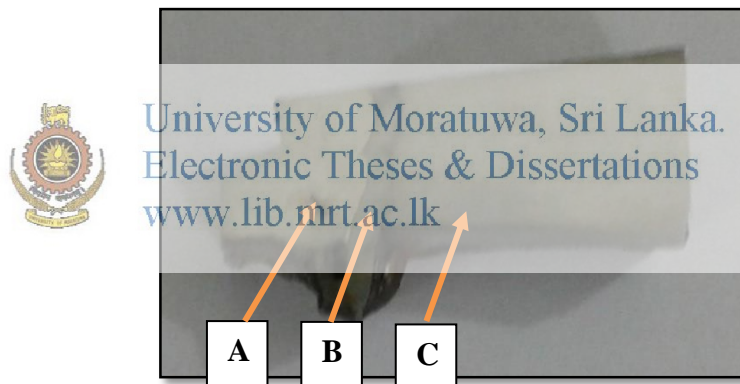


Figure 4.5 : Specimen of failed rudder



Figure 4.6 : Microstructure of all section of specimen -50X

Preparation of the specimen for micro level inspection was carried out initially using ferric chloride etchant. However, it was observed that metal A (portion of rudder blade) does not clearly visible with ferric chloride etchant. Then specimen was etched with Carpenter etchant which is suitable for austenitic stainless steel and the result was found to be satisfactory. Since, austenitic stainless steel has a strong anti-corrosive layer with the presence of high chromium and Nickel amount, it is harder to etch.



University of Moratuwa, Sri Lanka.
Electronic Theses & Dissertations
www.lib.mrt.ac.lk

Microstructures of section A, HAZ₁, B, HAZ₂ and C of the specimen are shown from figure 4.7 to 4.10 respectively.

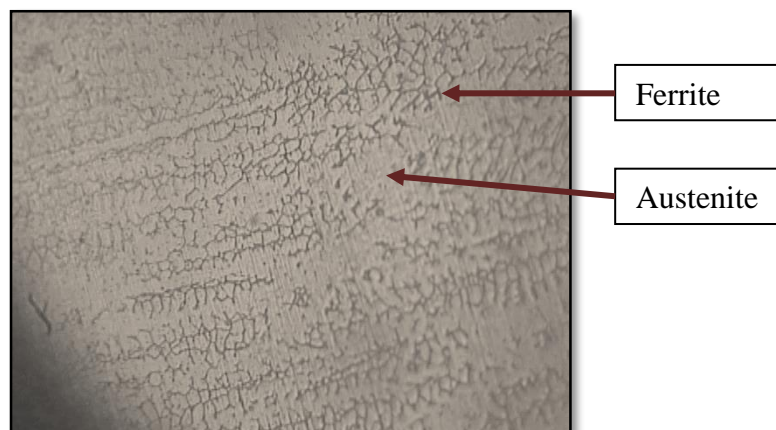


Figure 4.7 : Microstructure of Metal A - 400X

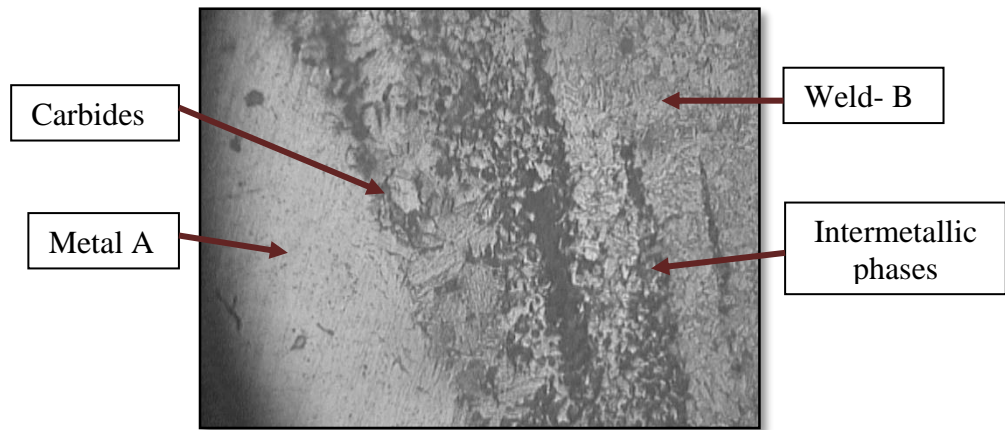


Figure 4.8 : Microstructure of HAZ₁ between metal A and weld B – 400 X



Figure 4.9 : Microstructure of Weld (B) – 400X

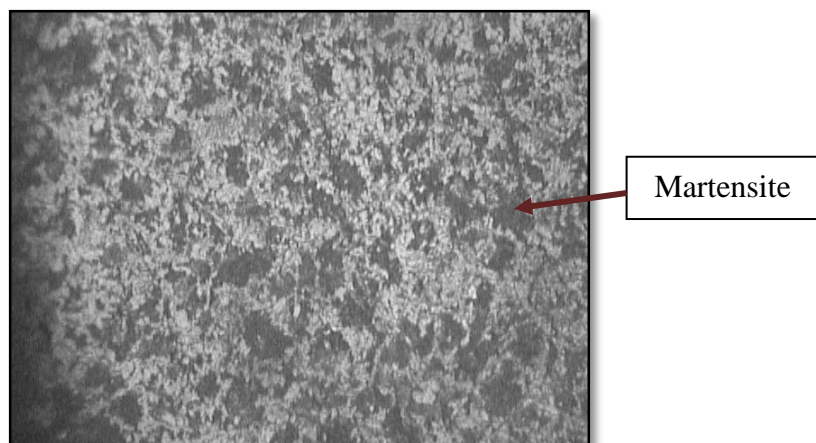


Figure 4.10 : Microstructure of HAZ₂ between Weld and Metal C – 400X

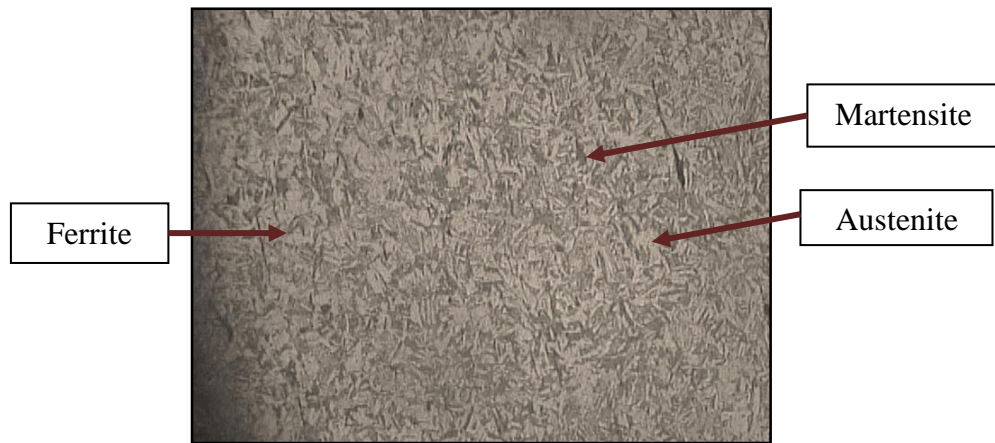


Figure 4.11 : Microstructure of Metal C – 400X

Phases presents in the above shown microstructures are as follows.

- a. Figure 4.7 – Microstructure of metal A is an austenite structure having delta ferrite in dark colour.
- b. Figure 4.8 – Microstructure of HAZ₁ between metal A and the weld. This microstructure contains intermetallic phases like sigma phases and carbides in dark colour.
- c. Figure 4.9 – Microstructure of weld metal is an austenite structure containing high amount of precipitated carbides and intermetallic phases.
- d. Figure 4.10 – Microstructure of HAZ₂ between weld and metal C. The structure consists of more martensite in dark colour.
- e. Figure 4.11– Microstructure of metal C. It is having austenite, martensite and ferrite structures.

4.1.3 Chemical Composition Analysis

The results of the chemical composition analysis of specimen is indicated in table 4.1

Table 4.1 : Chemical compositions of failed rudder materials

Element	Outer Section(A)	Weld(B)	Inner Section(C)
Cr	18.0	15.7	16.5
Ni	11.6	7.82	5.63
Mn	1.17	0.89	1.24
Mo	2.50	1.26	0.75
Si	0.23	0.14	0.19
P	0.015	0.011	0.021
C	0.06	0.32	0.04
S	0.002	0.018	0.001

The phases present on these metals were identified after plotting same on the Schaeffler Delong diagram and relevant diagram is shown at figure 4.12. The Chromium and Nickel equivalent of the failed rudder metals were calculated using following equations in order to plot metals into the diagram.

$$\text{Nickel equivalent} = \%Ni + 0.5x\%Mn + 30x(\%C + \%N)$$

$$\text{Chromium equivalent} = \%Cr + \%Mo + 1.5x\%Si + 0.5x\%Nb$$

Outer portion of the failed rudder stock (part of rudder blade) - A

Weld portion - B

Inner portion of the failed rudder stock(part of rudder stock) - C

Calculating Values for A Portion

$$Ni_{eq} = 11.6 + 0.5 \times 1.17 + 30 \times 0.06 = \underline{13.985}$$

$$Cr_{eq} = 18 + 2.5 + 1.5 \times 0.23 = \underline{20.845}$$

Calculating Values for B Portion

$$Ni_{eq} = 7.82 + 0.5 \times 0.89 + 30 \times 0.32 = \underline{17.865}$$

$$Cr_{eq} = 15.7 + 1.26 + 1.5 \times 0.14 = \underline{17.17}$$

Calculating Values for C Portion

$$Ni_{eq} = 5.63 + 0.5 \times 1.24 + 30 \times 0.04 = \underline{7.45}$$

$$Cr_{eq} = 16.5 + 0.75 + 1.5 \times 0.19 = \underline{17.535}$$

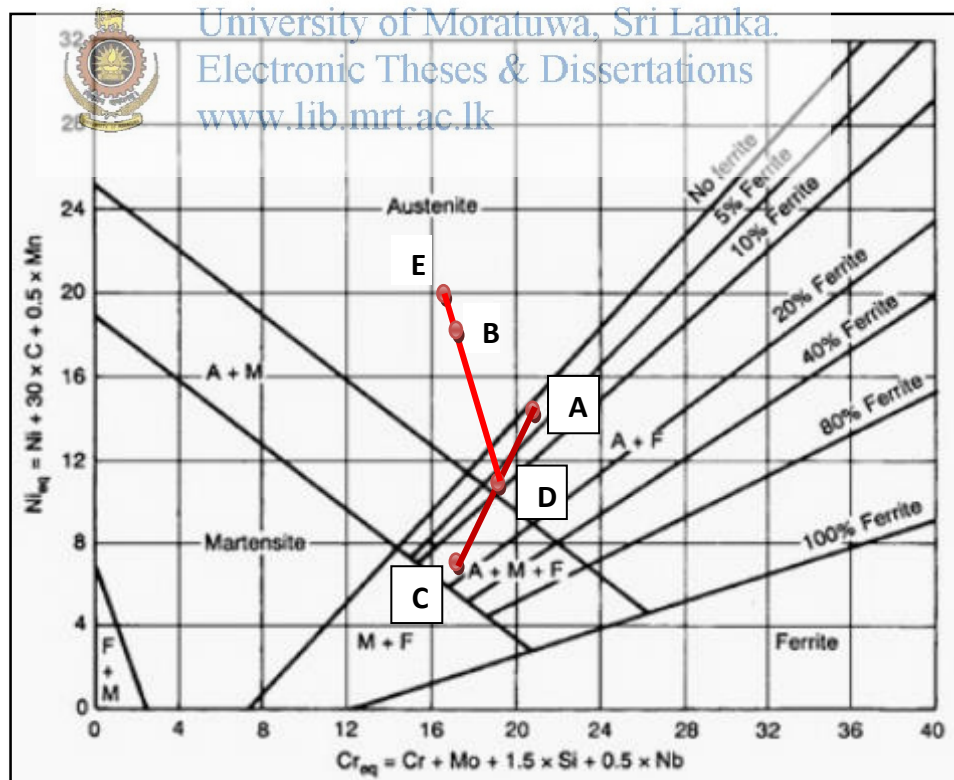


Figure 4.12 : Failed rudder materials floated on Schaeffler Delong Diagram

It was assumed that both base metals ‘A’ and ‘C’ are playing equal part for the weld and point ‘D’ is the equivalent of both base metals. Further, it was assumed 20% dilution between base metal and the welding electrode; point ‘E’ is the welding rod composition. Therefore, as per above Schaeffler Delong diagram it was revealed that base metal ‘A’ is having austenitic microstructure with about 2-3% ferrite, base metal ‘C’ microstructure having martensite and austenite with about 18% ferrite. Microstructure of weld ‘B’ is a complete austenitic structure.

Based on table 4.1 and figure 4.11, it was revealed that chemical composition of outer portion (rudder blade) and inner portion (rudder stock) of the rudder are different. Further, they belong to different stainless steel grades.

4.1.4 Micro Hardness Testing

The micro hardness readings of the specimen are indicated at table 4.2 and relevant graph is shown at figure 4.13.

Table 4.2 : Micro-hardness values of the sample
University of Moratuwa, Sri Lanka.

Distance (mm)	Hardness value (HV)	Distance (mm)	Hardness value (HV)
0.0	199.7	5.5	459.2
0.5	211.4	6.0	512.1
1.0	228.3	6.5	530.3
1.5	231.2	7.0	483.7
2.0	239.5	7.5	466.3
2.5	208.2	8.0	519.4
3.0	204.6	8.5	524.7

3.5	243.4	9.0	530.2
4.0	258.9	9.5	512.5
4.5	323.5	10.0	514.1
5.0	418.8		

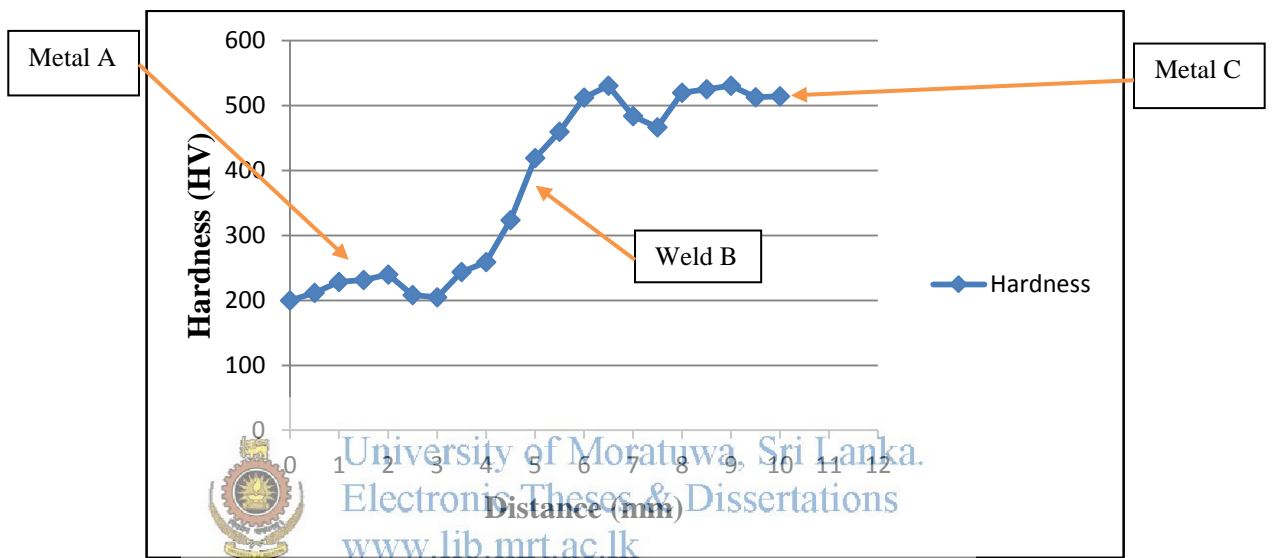


Figure 4.13 : Graph of micro hardness vs distance (failed rudder)

Micro hardness measurement values indicated at table 4.2 and the graph at figure 4.13 revealed that hardness of inner portion of the rudder (rudder stock) is very high compared to outer portion of the rudder (rudder blade). Therefore, metal used for rudder stock having more of martensitic microstructure.

Based on the macro/micro level inspection, chemical composition analysis and the micro hardness testing of failed rudder, it is revealed followings.

- a. Base metals used for rudder fabrication (metal A and metal C) are of dissimilar metals having different microstructure, different chemical compositions and different hardness. Therefore, these two base metals were behaved differently during fabrication process, especially during welding where metals are exposed to

high temperature; there are tendencies for carbide precipitation, formation of intermetallic phases and hot cracking.

b. Since, HAZ of the metal A was subjected to high temperature and welding electrode contain high percentage of carbon (0.32%), carbide precipitates in HAZ. Further, intermetallic phases such as sigma phases also formed in HAZ as metal A is having high Cr, Mo, Si content. Formation of carbides and intermetallic phases consumed considerable amount of Cr present in the metal. Therefore, in the HAZ of metal A toughness drops and corrosion resistance decreases. This is further substantiated by microstructure of HAZ₁ shown at figure 4.8.

c. The final weld is in complete austenitic region and it contains considerable amount of sulfur and phosphorous. Therefore, this weld is more susceptible to hot cracking as about 4 to 12 % of ferrite in the weld is essential to avoid hot crack.

d. Since metal C is having austenitic, ferritic and martensitic microstructures, HAZ of metal C is more prone to cracking as martensite phases produce hard martensitic zone adjacent to the weld which is brittle and less corrosion resistance. This is further substantiated by internal crack initiation shown at figure 4.2.

e. Since the rudder was subjected to low loading frequencies and craft was operated in severe corrosive environment, corrosion action was prominent near weld area. This is further substantiated by corroded area besides the weld shown at figure 4.4.

f. Stresses acting near the joint where the rudder blade joins the rudder stock are high having low cross section area at the joint. Therefore, with the internal crack initiation progress the crack across the shaft and for final sudden failure (figure 4.1).

g. Considerable porosities in the weld area (figure 4.4) also contributed to the failure by weakening the weld joint.

4.2 Analysis of Existing Rudder Fabrication Process

Examination of existing rudder fabrication process is discussed in subsequent sections.

4.2.1 Selection of Materials

Materials selection for in-house rudder fabrication was done without considering chemical compositions and other mechanical properties of stainless steels. Use of old propeller shafts for fabricating a rudder is not recommended as those shafts were used for number of years in severe corrosive environment and even subjected to different stresses during operation.

4.2.2 Welding Process

The arrangement of stainless steel shafts prior to welding is shown at figure 4.14. As per the arrangement, it was observed that root face of the weld joint is thin and it is not favorable as molten stainless steel weld metal is less fluid. Hence, less weld penetration create incomplete bond.



University of Moratuwa, Sri Lanka.
Electronic Theses & Dissertations
www.lib.mrt.ac.lk



Figure 4.14 : Arrangement of shaft prior to welding

As per the welding parameters indicated at section 3.3.2.3, metals were exposed to considerable temperature and time. Hence, it was created favorable condition for carbide precipitation during welding which is susceptible for intergranular corrosion.

Further, followings general practices of welders were created defects in the weld.

a. Welding electrodes which are kept exposed to atmosphere for longer period cause coatings of the electrode to absorb moisture which in turn create porosities during weld start. This is further substantiated by the figure 4.15 which shows porosities in sample weld piece.

b. Performing of welding and grinding processes repeatedly during the rudder fabrication until gets final finish and required dimensions, metals are susceptible for cracks formations.

c. Continuation of welding until completion of entire welding electrode, keeps the weld metal and HAZ hot over a longer period, allowing more time for precipitation of carbides or formation of intermetallic phases.



Figure 4.15 : Porosities on sample weld piece

4.2.3 Chemical Composition Analysis

Chemical composition analysis of material used for recently fabricated rudder is presented at table 4.3.

Table 4.3 : Chemical composition readings of new rudder metals

Element	Chemical Composition		
	Used shaft	Purchased shaft	Welding rod
Cr	18.7	19.2	18.7
Ni	14.69	10.4	12.65
Mo	3.12	-	2.3
Mn	1.85	1.9	1.75
Si	0.22	0.74	0.52
	0.1	0.08	0.035
S	0.008	0.03	0.022
P	0.009	0.04	0.024
other	Cu- 0.22	N- 0.1	

Chemical composition analysis of metals used for recently fabricated rudder was revealed that they are not the same stainless steel type. Further, used propeller shafts metal chemical composition includes 0.22% of Cu which promotes an austenitic microstructure and improve machinability/formability.

Chromium and Nickel equivalents of metals were calculated as follows in order to plot on Schaeffler Delong diagram and same shown at figure 4.16.

Calculating Values for Used Shaft (A₁)

$$Ni_{eq} = 14.69 + 0.5 \times 1.85 + 30 \times 0.1 = \underline{18.615}$$

$$Cr_{eq} = 18.7 + 3.12 + 1.5 \times 0.22 = \underline{21.832}$$

Calculating Values for Purchased Shaft (B₁)

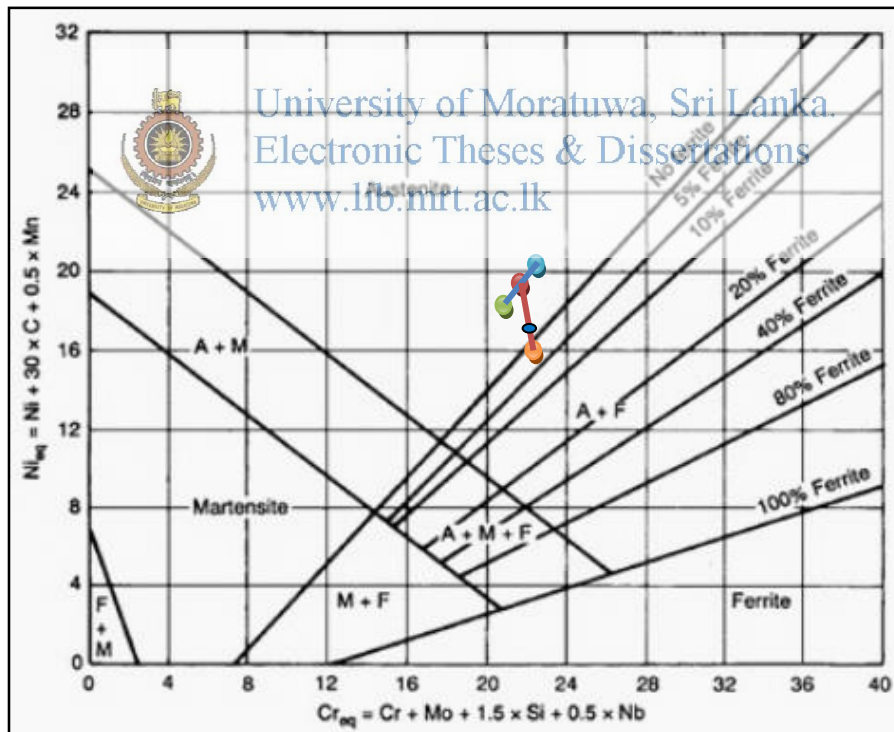
$$Ni_{eq} = 10.4 + 0.5 \times 1.9 + 30 \times (0.08 + 0.1) = \underline{16.75}$$

$$Cr_{eq} = 19.2 + 1.5 \times 0.74 = \underline{20.31}$$

Calculating Values for Weld Electrode (D₁)

$$Ni_{eq} = 12.65 + 0.5 \times 1.75 + 30 \times 0.035 = \underline{14.575}$$

$$Cr_{eq} = 18.7 + 2.3 + 1.5 \times 0.52 = \underline{21.78}$$



- A1- Used Shaft
- B1- Purchased Shaft
- C1- Equivalent Composition
- D1- Welding Electrode
- E1- Resultant Weld (with 30% dilution)

Figure 4.16 : Schaeffler Delong diagram for new rudder metals

Schaeffler Delong diagram at figure 4.16 revealed that resultant microstructure of the weld is in complete austenitic region. Further, both purchase shaft and welding electrode contain high amount of phosphorous and sulfur which create favourable situation for hot cracking.

Since used shaft material contain considerable high amount of carbon(0.1%), HAZ of used shaft material is more susceptible for carbide precipitation.

4.2.4 Microstructure Analysis

Microstructure of the heat affected zone (HAZ) of used shaft shown at figure 4.17 was revealed it contain coarse grains and a crack along the grains.



Figure 4.17 : Microstructure of HAZ of used shaft– 400X

4.2.5 Micro Hardness Testing

Micro hardness values of the sample shown at figure 4.18 was taken and indicated at table 4.4. The relevant graph is shown at figure 4.19.

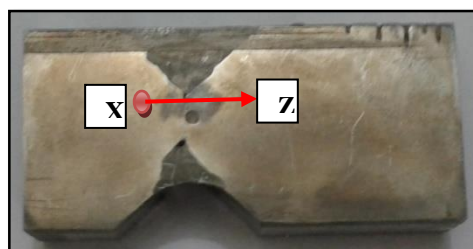


Figure 4.18 : Sample weld piece

Where;

X = Measurement starting point

Y = Measurement end point

Table 4.4 : Micro hardness values of the sample

Distance(mm)	Hardness value (HV)	Distance (mm)	Hardness value (HV)
0.0	183.9	6.5	198.2
0.5	189.4	7.0	192.6
1.0	191.5	7.5	201.4
1.5	195.3	8.0	200.5
2.0	200.5	8.5	202.1
2.5	201.2	9.0	198.8
3.0	202.5	9.5	196.4
3.5	198.4	10.0	180.2
4.0	190.7	10.5	170.7
4.5	172.6	11.0	165.2
5.0	186.0	11.5	178.6
5.5	187.6	12.0	182.5
6.0	191.3	12.5	184.2

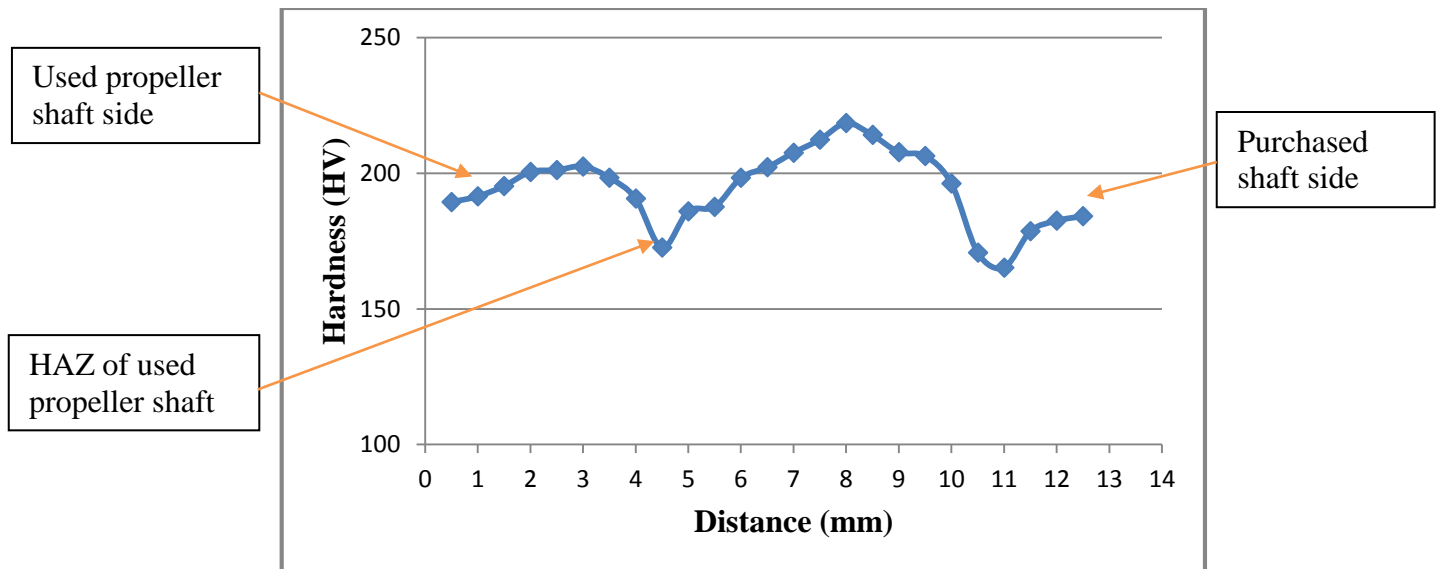


Figure 4.19 : Graph of micro hardness vs distance

Figure 4.19 was revealed that hardness of used propeller shaft is slightly higher compared to that of purchased shaft and hardness of HAZ of used propeller shaft drops.

Based on the material selection, monitoring of welding process, chemical composition analysis, microstructure analysis and micro hardness testing of existing rudder fabrication process was revealed followings.

a. Since used propeller shafts which were selected for fabricating the rudder is having high carbon content (0.1%) and welding parameters/general practice of welders creates favorable high temperature region, carbides precipitates at the grain boundaries of the HAZ of used shaft. Therefore, intergranular stress corrosion crack was initiated at the HAZ. This is further substantiated by microstructure of HAZ shown at figure 4.17.

b. Used shafts having high Molybdenum and silicon content promote formation of intermetallic phases during welding. Thus drop in toughness and decrease in resistance to corrosions.

c. Further, used propeller shafts chemical composition includes 0.22% of Cu which promotes an austenitic microstructure and improve machinability/formability. Therefore, it was understood that these shafts have been designed for specific application.

d. Since HAZ of the used shaft contained coarse grains, hardness values at HAZ drops compared to base metal. This is further substantiated by the figure 4.19.

e. Selected welding electrode was also not suitable as final weld lies in complete austenitic region which is susceptible for hot cracking.

4.3 Calculation of Cross Sectional Area of Weld Fill

Calculations of cross sectional area of the weld fill which was done for both 'U' and 'V' groove one half (section x) shown at figure 2.8 and figure 2.9 are as follows.

- Cross sectional area for 'U' groove (only for section 'x') = X
- Cross sectional area for 'V' groove (only for section 'x') = Y

Followings were assumed for calculation,

$$A = 45^\circ$$

$$B = 10^\circ$$

$$R = L/5$$

Where L is the height of the weld

$$Y = 1/2 \times L \times L \tan A$$

$$= \underline{\underline{0.8099L^2}}$$

$$X = 1/4\pi R^2 + R \times (L-R) + 1/2 (L-R)\tan B \times (L-R)$$

$$= \underline{\underline{0.3189L^2}}$$

Therefore, a 'U' groove (figure 2.8), which gives a smaller volume than a 'V' groove (figure 2.9) and in thicker plates (when L increases) this is more effective.


5. CONCLUSION

Fast attack craft rudder failed as a result of fatigue during the operation and following conclusions were drawn from the research.

- a. Base metals used for rudder fabrication (metal A and metal C) are of dissimilar metals having different microstructure, different chemical compositions and different hardness. Therefore, these two base metals behaved differently during fabrication process and the operation.
- b. Chemical compositions of the metals used for rudder fabrication and the temperature to which metals were exposed during welding lead to the creation of favourable environment for carbide precipitation and formation of intermetallic phases. Therefore, HAZs of the welds were susceptible for intergranular corrosion and same was accelerated by operating of craft in severe corrosive environment.
- c. The weld was more susceptible to hot cracking as it was in complete austenitic region and it contains considerable amount of sulfur and phosphorous.
- d. Crack was nucleated at the HAZ of the metal C (rudder stock) being an area which was brittle and less corrosion resistance. This is further substantiated by internal crack initiation as shown at figure 4.2.
- e. Considerable porosities in the weld area also weakened the weld joint.

6. RECOMMENDATIONS

Based on the research, followings are recommended in order to avoid this type of rudder failures in future.


- a. Stainless steels are designed by carefully balancing the alloying elements so that appropriate microstructure is maintained to use for specific applications. Therefore, in the selection of materials for fabricating of a rudder, attention must be paid to the application, service condition and the processes involved.
- b. Since, welding processes are heavily involved during the rudder fabrication; it is preferable to select similar stainless steel grades of low carbon content as base metal in order to avoid formation of carbides and intermetallic phases.
- c. Select welding electrodes such that final weld contains austenite microstructure with 4 to 12% of ferrite in order to avoid hot cracks.
- d.  Take extra precautions to prevent exposure of weld electrode to atmosphere as it creates room for formation of porosities in the weld.
University of Moratuwa, Sri Lanka.
Electronic Theses & Dissertations
www.lib.mru.ac.lk
- e. Perform welding processes so as to minimize re-welding and grinding processes as otherwise it may induce stresses at the weld.
- f. Preparation of uniform welding joints in order to ensure complete bond between metals.
- g. Take adequate measures to prevent longer exposure time for high temperatures of stainless steel during welding.
- h. Ensure proper cleaning prior to welding and in post welding using stainless steel tools such as stainless steel wire brushes etc.

References

- [1] A.S. A. Elmaryami and B. Omar, (2012). Heat Transfer Phenomena and Application, *Developing 1-Dimensional Transient Heat Transfer Axi-Symmetric MM to Predict the Hardness, Determination LHP and Study the Effect of Industrial Quenched Steel Bar*. [online], pp 154. Available : <http://dx.doi.org/10.5772/51947>.
- [2] D. Kotecki and F. Armao. Stainless Steel Welding Guide. Lincoln Welding Company, 2003. Available:
www.lincolnelectric.com/assets/globe/products/consumable_stainlessNickelandHighAlloy.pdf
- [3] W.D Callister and D.G Rethwisch. *Material Science and Engineering an Introduction*, 8th ed., Hoboken, NJ, 2009, pp. 319- 321.
- [4] V. Raghavan. *Material Science and Engineering*, 5th ed., New Delhi: PHI Learning Private Limited, 2010, pp. 328
- [5] H. Panthron (2012, May 5th) *Phase Transformations* *Chemical Engineering Daily Report* [online]. Available : www.lib.mrt.ac.lk www.chemicalengineeringdaily.blogspot.com
- [6] T. Fischer. *Material Science for Engineering Students*, Hoboken, NJ, Elsevier Inc. 2009, pp. 161
- [7] C.P. Sharma. *Engineering Materials, Properties and Application of Metals and Alloys*, Jaipur, New Delhi, Prentice Hall of India Private Limited. 2004, pp. 38.
- [8] F.C. Campbell, *Element of Metallurgy and Engineering Alloys*, Ohio, ASM International, 2008, pp 371.
- [9] V.B. Ginzburg and R. Ballas. *Flat Rolling Fundamentals*, New York, Marcel Dekker Inc. 2000, pp 36.
- [10] J.T.W. Jappes, A. Alavudeen and N. Venkateshwaran. *A Test book of Engineering Materials and Metallurgy*, New Delhi, India, LP, 2006. pp 103-105.

- [11] M. F. Mc Guire (2008, Jun 1). *Stainless Steel for Design Engineers*, [online]. Available :
www.asminternational.org/document/10193/3473958/05231G_sample.pdf
- [12] W. Bolton. *Engineering Materials and Technology*, 2nd ed., oxford, UK, Newnes, 1993. Pp 209.
- [13] Practical Guidelines for the fabrication of High Performance Austenitic Stainless Steels, IMO A publication, London, UK, 2014. Available :
<http://www.imoa.info/imoa-downloads/austenitic-stainless-steel.php>
- [14] Hand book on Stainless Steel, Outokumpu Stainless steel AB, Sweden, 2003. Pp 11-16.
- [15] Design guidelines for the Selection and use of Stainless Steel, Stainless Steel Information Centre, North America, 1988.
- [16] Welding of Stainless Steel and other Joining Methods. American Iron and Steel Institute, Washington, USA, 1979.
- [17] Some facts about Alloying and accompanying elements in steel. Special Steels Catalogue, Macsteel, South Africa. Available : www.macsteel.co.za
- [18] J.C.Lippold and D.J. Koteki. *Welding Metallurgy and Weldability of Stainless Steels*. John Wiley & Sons Inc., 2005.
- [19] Application data sheet-stainless steel, Austral Wright Metals, AW Distribution Pty Ltd, Australia, 2000. Available :
www.australwright.com.au/sensitization-of-stainless-steel
- [20] Role of grain boundary carbides in cracking behaviour of Ni based alloy, OAK Central, Korea, 2013. Available :
www.central.oak.go.kr/journallist/journaldetail.do
- [21] T. Ogawa and E. Tsunetomi.(1982). Hot Cracking Susceptibility of Austenite Stainless Steels. *Welding Research Supplement*. Pp- 1.

- [22] A. Moteshakker and I. Danaee. (2015, Nov). Microstructure and corrosion resistance of dissimilar weld-joints between duplex stainless steel 2205 and austenitic stainless steel 316L. *Journal of Material Science and Technology*. [online]. 32, pp 282-290. Available: ScienceDirect.
- [23] P. Sathiya, S. Aravindan, R. Soundararajan and A. N. Hag. *Material Science*. Hoboken, NJ, Elsevier Inc. 2009, pp 114-121.
- [24] Kobelco. (2002, Jan). “The ABC’s of Arc Welding, Hot Cracks” [online]. Available : <http://www.kobelco-welding.jp/education-center/abc/ABC-2002-01.html>
- [25] BOC Library, AU:IPRM:2007: Section 8, Consumable, pp 388 -419. Available : [http://www.bocworldofwelding.com.au/consumable/stainless steel.pdf](http://www.bocworldofwelding.com.au/consumable/stainlesssteel.pdf)
- [26] Stainless steel weld joints, Integrated publishing, China. Available : www.navyaviation.tpub/14018/css/14018-649.htm
- [27] S. Fisher, C.A. Oliver and S.T. Riches, Optimisation of plasma control parameters for Nd: YAG welding of stainless steel enclosures, 7th NOLAMP conference, Lappeenranta, Finland, 1999. Available : www.twi-global.com/technical-knowledge/published-papers
- [28] G. Magudeeswaran, V. Balasubramanian and G.M. Reddy, (2014). Effect of welding processes and consumables on fatigue crack growth behaviour of armour grade quenched and tempered steel joints. *Journal of Defence Technology*, [online]. pp 47-59. Available : ScienceDirect.
- [29] Hand book on Stainless Steel, Loc. Sit, pp 35-39.
- [30] V. Muthupandi, P.B. Sirinivasan, S.K. Seshadi, S. Sundaresan. *Material Science Engineering* Hoboken, NJ, Elsevier Inc. 2003, pp 9-16.
- [31] M.A.D. Aguilar and R.C. Newman. (2006). Formation of intermetallic phases and effect on corrosion resistance of austenitic stainless steel. *Journal of corrosion resistance*. [online]. pp 2560-2576. Available : ScienceDirect.

- [32] G. Sui, E.A. Charles and J. Congleton.(1996). The effect of delta-ferrite content on the stress corrosion cracking of austenitic stainless steels in a sulphate solution. *Journal on corrosion science*,Vol.38, pp. 687-703. Available : ScienceDirect.
- [33] C.A.P. Horton, P. Marshall and R.G. Thomas, Time-dependent changes in microstructures and mechanical properties of type 316 steel and weld metal. *International Symposium. On Environment degradation of materials in Nuclear power systems- water reactors*, p.66. Myrtle Beach, South Carolina (1983).
- [34] L. Dong, Q. Peng, E.H. Han, W. Ke and L. Wang.(2016). Stress corrosion cracking in the heat affected zone of a stainless steel 308L-316L weld joint in primary water. *Journal on corrosion science*,Vol.107, pp. 172-181. Available : ScienceDirect.
- [35] Det Norske Veritas. (2000, Jun). “Casualty Information” [online]. Available : <http://www.officerofthewatch.com>
- [36]  Mathew Sheahan. (2015, Mar). “Yachting World” [online]. Available : <http://www.yachtingworld.com/features/rudder-failure-in-the-med>.
 University of Moratuwa, Sri Lanka.
 Electronic Theses & Dissertations
www.lib.moratuwa.lk
- [37] Jenny. (2014, Jun). “SV Full Monty” [online]. Available : <http://www.svfullmonty.com/2014/06/10/tonga-lost-a-rudder>.